How do the mechanical demands of cycling affect the information content of the EMG?

James M. Wakeling[1] and Emma F. Hodson-Tole[2]

[1]Department of Biomedical Physiology and Kinesiology, Simon Fraser University, Burnaby, BC, Canada

phone 1-778-7828444

fax 1-778 7823040

wakeling@sfu.ca

[2]School of Healthcare Science, Manchester Metropolitan University, Manchester, United Kingdom

Accepted for publication in Medicine and Science in Sports & Exercise (2018)

Published ahead of print at: https://journals.lww.com/acsm-msse/Abstract/publishahead/How_Do_the_Mechanical_Demands_of_Cycling_Affect.96864.aspx

doi: 10.1249/MSS.0000000000001713

Abstract

Purpose: The persistence of phase-related information in EMG signals can be quantified by its entropic half-life, EnHL. It has been proposed that the EnHL would increase with the demands of a movement task, and thus increase as the pedalling power increased during cycling. However, simulation work on the properties of EMG signals suggests that the EnHL depends on burst duration and duty cycle in the EMG that may not be related to task demands. This study aimed to distinguish between these alternate hypotheses. **Methods:** The EnHL was characterized for 10 muscles from nine cyclists cycling at a range of powers (35 to 260 W) and cadences (60 to 140 r.p.m.) for the raw EMG, phase-randomized surrogate EMG, EMG intensity and the principal components describing the muscle coordination patterns. **Results:** There was phase-related information in the raw EMG signals and EMG intensities that was related to the EMG burst duration, duty cycle pedalling cadence and power. The EnHLs for the EMG intensities of the individual muscles (excluding quadriceps) and for the coordination patterns decreased as cycling power and cadence increased. **Conclusions:** The EnHLs provide information on the structure of the motor control signals and their constituent motor unit action potentials, both within and between muscles, rather than on the mechanical demands of the cycling task *per se*.

Key words: Sample entropy, entropic half-life, principal component analysis, skeletal muscle, coordination, firing statistic

Introduction

The EMG signal represents the superposition of motor unit action potentials from activated motor units and is commonly assessed to identify characteristics such as firing rates of individual units (1) or recruitment of populations of units (2). Within an individual muscle, more generalized features of activity, such as the time of onset and offset and the magnitude of each burst, can also be determined from fluctuations in the intensity envelope of the EMG recorded during activities such as cycling. Additionally, the coordination of multiple muscles within each limb can also be assessed and has been shown to be a key determinate to cycling performance (3).

However, the structure (temporal organization of variability) within the EMG signal may also contain information on the challenge posed by a movement task and give us new insight to the motor control strategies that govern the muscles to meet these challenges. One way to determine the structure of a signal is to calculate its Entropy (4), and for EMG signals this can be done using a particular approach termed Sample Entropy. Sample Entropy (5) identifies how often small segments of data (with m sample points) from a signal would be identified within the signal (within a specified tolerance) compared to segments that contained one more (m+1) sample point. A low value of Sample Entropy reflects a high degree of structure in the signal, with higher Sample Entropy reflecting a more chaotic structure. This approach was further developed (6) and has been used to quantify the rate at which signal structure decays within EMG signals (7) using a measure termed the entropic half-life, EnHL. Calculation of EnHL involves resampling the original EMG signal at increasingly larger time steps, to identify the time-scale at which structure in the signal is lost as the resampled signal transitions to containing random fluctuations.

Muscle activity during cycling varies with both cadence and power (3, 8-15). When increasing the pedalling cadence the burst duration decreases (8) but not as much as the cycle duration, and so the duty cycle increases. All EMG signals recorded during cycling have structure reflecting the neuromuscular control of their motor units, and a theoretical analysis of the factors that shape surface EMG signals and their effect on EnHLs predicted that EMG signals at the fastest cadences (short burst durations and longer duty cycles) would result in shorter EnHLs (7). However, this is contrary to the view that high-cadence cycling represents a demanding task that would result in greater, or more persistent, structure to the neuromuscular control strategy. Whether EMG signal structure during cycling reflects structure to the neuromuscular control strategy is therefore not clear. We therefore aim to address this gap in knowledge by investigating structure of raw EMGs, EMG intensity and muscle co-ordination patterns and how EnHL changes in response to cycling demand. Below we provide a rationale for why each signal may be expected to be structured and the physiological responses to the cycling demand that may influence that structure.

Within the raw EMG each motor unit action potential occurs at a distinct time and leaves characteristic spectral components in the EMG signal (16). If the variability in the EMG signal is organized over time (i.e. it is structured) the action potential shapes, amplitudes and the relative phase between different motor units potentials' would be expected to influence the characteristics of the structure. As motor unit recruitment responds to the mechanical demands of cycling (17), changes in raw EMG signal structure would be predicted to occur in response to altered cycling mechanical demands.

The EMG intensity provides an envelope of the signal, smoothing out some of the time-dependent fluctuations from the raw EMG signal. It is therefore possible that EMG intensities from individual muscles may be more structured (i.e. fewer random fluctuations) than the raw EMG. This

may mean that burst parameters within each muscle, such as burst duration and duty cycle, are the main factors influencing the individual EnHLs. Cycling at higher cadences results in decreased burst duration (8), and higher duty cycles, that have led to predictions of shorter EnHLs (7). These predictions have yet to be tested on experimental data.

Muscle coordination patterns that consist of the EMG intensities from many different muscles may show greater variability due to the higher-dimensionality of the additional muscles, and so the EnHLs for coordination may be shorter than for the individual muscles as the more variable structure of the coordination may dissipate over shorter time scales. EnHLs from such multi-muscle coordination patterns may reflect the net response of the neuromuscular system and may therefore provide insight into the structure of variability of muscle recruitment patterns tolerated by the nervous system for different task demands. Enders et al. (18) showed an increase in EnHL from 9 ms to 16 ms between 150 W and 300 W power conditions for cycling at 90 r.p.m. However, it is not known if this finding can be generalized across a range of cycling conditions particularly as the variability in and composition of the muscle coordination during cycling depends in a complex and non-linear fashion on both the power output and the cadence (8).

The purpose of this study was thus to explore the EnHL from the level of the raw EMG signal through to multi-muscle co-ordination patterns during cycling. We address the question of whether the EnHLs at these different signal levels vary with the opposing demands of the cycling task (high power output and cadence), or with EMG parameters (burst duration and duty cycle).

Methods

The entropic half-life, EnHL, was determined from a large cycling data set that has been described in a previous study (15). In brief, nine club to national level racing cyclists pedaled on an indoor ergometer at a range of cadences (60, 80, 100, 120 and 140 r.p.m.) at a low and fixed crank torque of 6.5 N m, and also cycled at a range of crank torques (12.9, 25.1, 32.4 and 39.9 N m) at the low cadence of 60 r.p.m. Cyclists pedaled for 5-10 seconds to reach a steady-state speed, and then data were recorded for a further 30 s for each trial. The cycle conditions were presented in a random order, and repeated in three blocks in order to minimize bias due to increasing fatigue and body temperature. A total of 6804 pedal cycles were analyzed (9 subjects x 3 blocks x 9 conditions x 28 cycles per condition). Pedalling cadence was maintained using visual feedback, and independently recorded with a pedal switch; post analysis showed it was on average 1.3 r.p.m. higher than the target velocity, and varied with a standard deviation of only 1.1 r.p.m. within each trial; there was a slight increase in variability in pedal cadence at the higher cadences, with the 140 r.p.m. trials having standard deviations of 1.8 r.p.m.. A 45 s rest period was given between each condition. Each participant gave written informed consent in accordance with the Simon Fraser University's policy on research using human subjects.

Bipolar Ag/AgCl surface EMG electrodes (10 mm diameter, 21 mm interelectrode distance) were placed in the centre of the muscle bellies of the tibialis anterior (TA), medial gastrocnemius (MG), lateral gastrocnemius (LG), soleus (Sol), vastus medialis (VM), rectus femoris (RF), vastus lateralis (VL), biceps femoris long head (BF), semitendinosus (ST), and gluteus maximus (Glut) of the left leg and surface EMG was recorded at 2000 Hz. A pedal switch allowed the time of top-dead-centre to be identified.

The entropic half-life, EnHL, was calculated for each signal using the following procedure. Initially the EnHL was calculated from the raw EMG signals (as directly recorded from the EMG amplifiers). These signals were filtered (Butterworth, high-pass with 10 Hz cutoff) and standardized to

126 have a mean of zero and standard deviation of one. The SampEn was calculated using a freely available
127 software package (19). SampEn(*m, r, N*) quantifies the regularity of a time series of length *N*, reflecting
128 the conditional probability that two sequences of *m* consecutive data points, similar to one another
129 within a tolerance (*r*), will remain similar when a consecutive data point is added (20). Values of *m*=0
130 and *m*=1, were recorded with *r*=0.2 for a range of reshape-scales from 1 ms to 1 s (6). For each reshape-
131 scale, the SampEn for *m*=1 was normalized to the corresponding SampEn for *m*=0 (which can be
132 interpreted as the negative logarithm of the probability of a match of length one (19)): this stage is
133 computationally faster but equivalent to normalizing to the random permutation of the signal as
134 described by Enders and co-workers (18). EnHL is the time-scale at which the normalized SampEn
135 (from across the reshape-scales) reached a value of 0.5 (18), indicating the time-scale that the time series
136 transitioned from ordered to random structure. It therefore provides a measure of the persistence of
137 structure in the EMG intensity envelopes from each individual muscle.

138 The intensity envelope for the EMG signals was calculated for each muscle, using an EMG-
139 specific wavelet analysis (21), where each wavelet k had a centre frequency $f_c(k)$, and the sum of the
140 intensities i_k over the frequency band 11 to 432 Hz ($1 \leq k \leq 10$) generated the total intensity that was a
141 close approximation to the power within the EMG signal. The mean frequency f_m for the EMG intensity
142 (16) was:

143 $$f_m = \frac{\sum_k f_c(k) i_k}{\sum_k i_k}$$

144 The EMG intensities for each muscle and trial were mean normalized and each intensity trace was
145 resampled at 1000 Hz. The burst durations for the normalized EMG intensities were taken as the
146 duration that the intensity was greater than 5% of the maximum for each pedal cycle, and the duty cycle
147 was the proportion of this burst duration relative to the period of each pedal cycle. The mean frequencies

of the EMG intensities were calculated for each pedal cycle. EnHLs were calculated for the EMG intensities in the same manner as describe above for the raw EMG signals.

The muscle coordination patterns were quantified by principal component analysis. For each cycling trial the coordination patterns for each time instant were generated from the normalized EMG intensities for all ten muscles, and placed in an $p \times N$ matrix $\boldsymbol{A}$ (p = 10 muscles, N is number of time points for 28 pedal cycles at the 1000 Hz sample rate). The mean intensity vector (mean intensity for each muscle in $\boldsymbol{A}$) was subtracted from $\boldsymbol{A}$, from which the covariance matrix $\boldsymbol{B}$ was calculated. The principal components, PCs, of $\boldsymbol{A}$ were described by Eigen analysis of $\boldsymbol{B}$: the PC loading scores were calculated from $\xi'\mathbf{A}$, where ξ' are the transpose of the Eigen vectors of $\boldsymbol{B}$ and were ordered into decreasing Eigen values. The loading scores for the first six PCs explained 91 % of the variance within matrix $\boldsymbol{B}$, and were used as signals for the EnHL analysis, as above, providing a measure of the persistence of structure in the multi-muscle coordination patterns.

The EnHL was additionally calculated for phase-randomized surrogates (18) of the raw EMG signals and the EMG intensity envelopes for each muscle and each trial. Phase-randomized surrogate signals have the same power spectrum and auto- correlation as the original signal; however, the structure encoded in the phase is removed. The process of phase-randomization removes structure due to the bursting patterns of the EMG, due to regularity of firing or synchronization of the motor units, and from the shape of the individual motor unit action potentials (Fig. 1). Thus, the surrogate signals can be used as reference values for signals with no structure (18).

The factors influencing the EnHL values were tested using mixed model analyses of covariance (Minitab version 16, State College, PA): cadence, power, burst duration, duty cycle and EMG intensity were included as covariates, and subject was a random factor. ANCOVAs were evaluated for the EnHL

for the raw EMG and for the EMG intensities, and these used the muscle as an additional factor and muscle × power, cadence × power and muscle × cadence as interaction terms. A third ANCOVA was evaluated for the EnHL for PC loading scores, and this used the PC number as an additional factor, and PC number × power, cadence × power and PC number × cadence as interaction terms. For this ANCOVA the burst duration, duty cycle and EMG intensity values used as covariates were taken as the mean values across the ten muscles. Statistical effects were deemed significant at $p<0.05$, and data are reported as mean ± standard error of the mean.

Results

The cycling conditions encompassed a range of powers, of which a set was at a low-cadence of 60 r.p.m. but at increasing crank torques, whilst a second set was at a low crank torque but with increasing cadence. There was a general increase in EMG intensity for each muscle with power, with greater EMG intensities occurring for the higher-cadence conditions for each given power (Fig. 2A). There was a cadence-specific effect on the burst durations with shorter burst durations occurring for faster cycling cadences (Fig. 2B). There was a general but small increase in duty cycle with power for all muscles (Fig. 2C).

The mean EnHLs for each muscle for the phase-randomized surrogate EMGs ranged between 5.23 ± 0.04 to 9.05 ± 0.05 ms ($N = 269$). These EnHLs showed a strong negative correlation with the mean frequency of the EMG intensities ($r^2 = 0.94$; Fig. 3A), with even higher correlations occurring ($r^2 = 0.98$) when the EnHLs for the phase-randomized surrogate EMG intensities were correlated against the period of the mean frequencies (1 / mean frequency) of the EMG intensities.

191 The mean EnHLs for each muscle for the raw EMGs were typically greater than their phase-
192 randomized values and ranged between 1.32 ± 0.10 and 45.64 ± 5.50 ms ($N = 28$) for the least
193 demanding condition of 60 r.p.m. at 35 W. The mean EnHLs for each muscle for the raw EMGs showed
194 a general decrease at the higher cadences when the torque was held constant (Fig. 4A). As the torque
195 increased for the low cadence conditions there was an increase in EnHL for the raw EMG signals for
196 VM, RF, VL and Glut, with a decrease for the remaining muscles (Fig. 4B). The EnHLs for each muscle
197 for the raw EMGs neither correlated with the EnHLs for the phase-randomized raw EMGs ($0.01 < r^2 <$
198 0.15), nor with the mean frequency of the EMG intensities ($0.01 < r^2 < 0.10$; Fig. 3B).

199 The EnHLs for the EMG intensities ranged between 20.26 ± 1.40 and 36.70 ± 1.67 ms ($N = 28$)
200 for the least demanding condition of 60 r.p.m. at 35 W. There was a general decrease in the EnHLs to
201 values between 17.98 ± 0.59 and 24.16 ± 0.38 ms as power output increased for both the increasing
202 torque and increasing cadence conditions, with the EnHL being more sensitive to changes in cadence
203 than crank torque (Fig. 5). However, the exception to this was the quadriceps muscles that increased
204 their EnHLs for the increasing torque conditions to reach their maxima, between 32.81 ± 1.80 and 35.71
205 ± 1.44 ms, at the 260 W power. The ANCOVA showed that decreases in EnHL were significantly
206 associated with increases in both cadence and power, and the EnHL showed a significant negative
207 association with EMG intensity and duty cycle, and a positive association with burst duration (Table 1).
208 The mean EnHLs for the EMG intensities for each muscle were greater than the mean EnHLs for the
209 intensities of the phase-randomized surrogate EMG and correlated with neither the mean frequencies of
210 the EMG intensities ($r^2 < 0.01$), nor with the EnHLs for the intensities of the phase-randomized signals
211 ($r^2 < 0.01$).

212

Table 1. Statistical results for the ANCOVAs. Columns show the effect of the covariate (up/down arrow indicate positive/negative direction of effect; - indicates no significant effect), the degrees of freedom (DF), *F*-value and *p*-value for the tests. Rows show the sources of variation: factors (subject: random; PC number and muscle), covariates (cycling cadence and power; EMG intensity; burst duration (BD) and duty cycle (DC)), interaction terms, and the error term.

	Raw EMG				EMG intensity				Muscle coordination			
	Covar.	DF	*F*	*p*	Covar	DF	*F*	*p*	Covar	DF	*F*	*p*
Subject		9	16.17	<0.001		9	10.29	<0.001		9	30.90	<0.001
PC #										5	3.51	0.004
Muscle		9	53.26	<0.001		9	20.32	<0.001				
Cadence	-	1	1.29	0.256	↓	1	9.58	0.002	↑	1	6.17	0.013
Power	↑	1	8.43	0.004	↓	1	20.44	<0.001	-	1	0.21	0.648
Intensity	↑	1	304.0	<0.001	↓	1	17.89	<0.001	-	1	0.29	0.587
BD	↑	1	14.12	<0.001	↑	1	52.97	<0.001	↑	1	4.59	0.032
DC	↓	1	22.37	<0.001	↓	1	195.39	<0.001	-	1	0.93	0.335
Muscle × Power		9	31.84	<0.001		9	41.45	<0.001				
Muscle × Cadence		9	24.65	<0.001		9	6.38	<0.001				
Cadence × Power		1	5.33	0.021		1	30.63	<0.001		1	7.10	0.008
PC # × Power										5	1.40	0.222
PC # × cadence										5	9.52	<0.001
Error		2606				2636				1579		

The EnHLs for the PC loading scores describing the muscle coordination patterns were shorter than the EnHLs for the EMG intensities for the individual muscles (Fig. 6). The EnHLs for the muscle coordination patterns ranged between 14.81 ± 1.22 and 21.80 ± 1.81 ms ($N = 28$) for the least

222 demanding condition of 60 r.p.m. at 35 W. The ANCOVA (Table 1) showed significant interaction
223 effects PC number, with the higher PCs resulting in lower EnHLs (Fig 5A). The EnHLs increased with
224 burst duration, and a significant interaction between PC number × cadence showed a greater cadence
225 dependence for the higher PCs (Fig. 6A).

226

227 **Discussion**

228 *Is there information in the EMG signal related to EnHL?*

229 The entropic half-life analysis in this study shows that there is persistent and non-random structure in all
230 levels of the EMG signals analysed, indicating that further investigation of structure in EMGs is
231 warranted. The phase of a signal has been shown to contain important information (22). At the level of
232 the raw EMG this may reflect the shapes of the MUAPs, variability (or lack-of) in the firing rates of the
233 motor units and coherence between different motor units. The raw EMG signals typically had longer
234 EnHLs than their phase-randomized surrogates (Fig. 3), so there is information in the phase properties of
235 the EMG. The EnHL for the phase-randomized signals correlated with the mean frequency of the EMG
236 and is of similar time-scale to the period of that mean frequency. This suggests that the fundamental
237 presence of voltage fluctuations (from the motor unit action potentials that make up the raw EMG) that
238 occur at distinct times and with distinct frequency properties, manifest as time-dependent structure to the
239 phase within that signal. Each motor unit action potential occurs at a distinct time and leaves
240 characteristic spectral components in the surface EMG signal (16) and these can also be resolved using
241 time-frequency signal processing techniques such as wavelet analysis (21, 23). The raw EMG had more
242 persistent structure (longer EnHLs) than the phase-randomized surrogate signals, but these EnHLs no
243 longer correlated with the mean frequency of the EMGs (Fig. 3B). Thus the additional structure within

the raw EMG derived from other features that are likely to include variability in the discharge of individual motor units (24-25), synchronicity between motor units (26) and activation-deactivation burst duration and duty cycle. This persistent structure and thus information in the raw EMG (Fig. 4) was also found in the individual muscle EMG intensity envelopes (Fig. 5) and in the multi-muscle co-ordination patterns (Fig. 6), although the timescale over which structure persisted and the changes in response to cycling demand differed. The factors that may cause these differences are therefore considered below.

Why does EnHL differ between the EMG signals analysed?

The raw surface EMG signals are the superposition of motor unit action potentials in the underlying muscle. Frequency information in the raw signal is strongly correlated with EnHL, even when the EMG is phase-randomized, and this information reflects the time-varying voltage fluctuations of the constituent motor unit action potentials. The raw EMG signals and the EMG intensities additionally contain phase-related information seen by their EnHLs being longer than their phase-randomized surrogates. EMG signals are the convolution of the firing statistics and the time-varying properties of the individual MUAPs, and so additional information in the EnHLs for the EMG intensities likely derives from the structure and variability in the firing. This structure is related to the discharge of individual motor units and synchronicity between motor units, both of which vary with activation levels and the proficiency for doing tasks. Whilst the EnHL for the EMG intensities was related to the burst durations for the EMG, they were considerably shorter than for those burst durations, and so fluctuations in the firing statistics are more rapid than each burst of activity.

The EnHL values from the EMG intensities of individual muscles were generally longer than those for the raw signals, likely reflecting smoothing out some of the time dependent fluctuations in the raw EMGs when the envelope of the signal is calculated. This means that burst parameters, such as

duration and duty cycle, may dominate the structure of the EMG intensity signal and indeed ANCOVA revealed a negative associations between EnHL and duty cycle, and a positive association between EnHL and burst duration (Table 1); and this is consistent with changes in EnHL that were simulated across this physiological range (7). It is these changes in burst duration that appear to play the major role in affecting the EnHL in these EMG intensities. It is of note that the burst durations (177.4 – 526.8 ms) were an order of magnitude greater than the EnHL values (15.7 – 36.7 ms; Fig. 5), and thus the reason for the reduced EnHL is probably not limited by the actual burst duration.

In the quadriceps muscles, however, there were longer EnHLs in the raw EMGs than in the EMG intensities in some cycling conditions. Structure persisted over longer time periods within the raw signals from these muscles when compared to others (Fig. 4), and this structure must have been related to time dependent fluctuations in the raw EMGs that were removed when the intensity envelope was calculated. The significance of these differences is difficult to determine from the data available from this study, but it is interesting to note that these muscles were the only ones in which significant changes in EnHL occurred between cycling conditions (greater EnHL associated with increasing torque conditions). It could be suggested that differences in motor unit (e.g. size, spatial distribution) and muscle anatomical (e.g. size, fibre pennation angle) features could combine to influence the raw EMG signals and hence EnHLs. However, similar EnHL values occurred across all muscles for some of the cycling conditions (e.g. Fig. 4), suggesting that the raw EMG signal properties altered in response to task demand. Important time-varying differences in the neuromuscular drive across individual muscles may therefore occur in response to task demands. These may reflect differences in the neuromuscular control required to elicit different mechanical roles of each muscle over the time course of a task (e.g. power production, force transfer**),** the dynamics of which warrants further investigation.

No muscle works in isolation, however, and as such it is valuable to consider the amalgamated responses of multiple muscles to task demand. Here, this was done by combining the intensity traces into multi-muscle coordination patterns, quantified by their PC loading scores, which resulted in EnHLs that were shorter than the EnHLs for the individual muscles. This was as expected, because the more muscles that are amalgamated into coordination patterns the more ways in which those patterns can vary, or the greater the chance the signal structure will dissipate. The EnHLs for the coordination calculated from this study are generally longer than those reported by Enders et al. (18), however, the calculated EnHLs are sensitive to the filter cut-off frequencies used before the sample entropy analysis: in this study the data were low-pass filtered with a 10 Hz cut-off due to the pedal cadences reaching 140 r.p.m., as opposed to the Enders et al. (18) study where a 2.5 Hz was used related to the cadence of 90 r.p.m..

Why does EnHL differ across cycling conditions?

Variability is a ubiquitous and fundamental characteristic of human movement (27), however variability may decrease with task constraints such as maximizing power output or pedalling velocity. Previous studies have shown that the dimensionality of muscle coordination patterns reduces for pedalling at greater power outputs (18, 28), and the variability of the muscle coordination patterns reduces at high cadences (8). However, the approaches used in those studies did not consider the temporal organization of variability that can be studied using the EnHL approach. Specifically, by analyzing the structure of signals over the time-course of the whole trial EnHL includes consideration of how one pedal cycle impacts subsequent cycles (i.e. effects of the order of data points across multiple pedal cycles is conserved in the analysis). The EnHL for the EMG intensities for the quadriceps muscles increased with power output for the low cadence, with increasing torque conditions. However, the EnHL for the remaining muscles, and for the increasing cadence conditions, showed general decreases with both power and cadence (Fig. 5). While the average variability of muscle coordination decreases with

311 greater task demand (8, 18, 28), the data presented here suggest that the time dependent structure of
312 these coordination patterns has greater variability during more challenging movement tasks. The shorter
313 EnHLs recorded may reflect greater interference, or more frequent adjustments, from the central nervous
314 system or may suggest that during more challenging tasks the nervous system was more tolerant of time-
315 varying fluctuations in coordination patterns; as has been suggested for postural balance tasks (29-30).
316 Further assessment of the temporal structure of variation in muscle co-ordination patterns and changes in
317 response to task demand are therefore warranted.

318 Previously, the EnHL for muscle coordination patterns has been shown to increase for cycling at
319 higher power output (18). The muscle coordination patterns were calculated from the time-varying EMG
320 intensities from seven lower extremity muscles that included three of the quadriceps, and it was found
321 that the principal coordination pattern for the high-power condition was dominated by signal from the
322 rectus femoris (18). In our current study the rectus femoris was one of the muscles that showed an
323 increase in EnHL as crank torque increased (Fig. 5B). However, the coordination patterns determined
324 here contain signals from 10 muscles, of which the majority did not show increases in EnHL with power
325 (Fig. 5). Furthermore, due to the large number of different conditions that we tested, we calculated a
326 common set of principal coordination patterns across all conditions: whilst such patterns are influenced
327 by the variability in the EMG intensity from the rectus femoris, the other muscles still have substantial
328 contribution across all principal patterns that are identified (8) and these muscles showed decreasing
329 EnHL with increased power output. These methodological differences explain the finding in this study
330 that the EnHL for the muscle coordination patterns did not increase with the increasing power (at a fixed
331 cadence) conditions.

332 It is possible that the EnHLs (for both individual muscles and for the coordination between
333 muscles) would have showed greater increases related to the increased demands of cycling at higher

power outputs than those tested in this study. It should be noted that the highest power tested in this study (260 W) is considerably less than the maximum powers that can be achieved by competitive cyclists (of over 1000 W; (31)) and so may have only been of limited challenge to the cyclists tested. Additionally, the relative intensities of the cycle conditions were not normalized to the maximum power achievable by each participant, and so the relative demands of the conditions may also vary between the cyclists tested.

We therefore conclude that there is structure at all levels of the EMG signals analysed here, with the persistence of this structure differing between muscles and in response to cycling task demand. Differences in structure relate to the underlying motor unit recruitment patterns and interacts with the electromyogram burst parameters. Further work is however required to determine the functional significance of the changes found here and to improve understanding of neuromuscular control of time dependent changes in muscle recruitment during dynamic tasks.

Acknowledgements

We thank Tamara Horn for assistance during the original data collection.

Conflicts of Interest and Source of Funding: There are no professional relationships with companies or manufacturers to disclose for all authors.

This research was supported by the Natural Sciences and Engineering Research Council of Canada. The results of the present study do not constitute endorsement by the American College of Sports Medicine.

The authors declare that the results of the study are presented clearly, honestly, and without fabrication, falsification, or inappropriate data manipulation.

355 **References**

356 1. De Luca CJ, LeFever RS, McCue MP, Xenakis AP 1982 Control scheme governing
357 concurrently active human motor units during voluntary contractions. *J Physiol* 1982; 329: 129–142.

358 2. Hodson-Tole E, Wakeling JM. Variations in motor unit recruitment patterns occur within and
359 between muscles in the running rat (*Rattus norvegicus*). *J Exp Biol* 2007; 210: 2333-2345.

360 3. Wakeling JM, Blake OM, Chan HK. Muscle coordination is key to the power output and
361 mechanical efficiency of limb movements. *J Exp Biol*. 2010; 213: 487–492.

362 4. Yentes JM, Hunt N, Schmid K, Kaipust J, McGrath D, Stergiou N. The appropriate use of
363 approximate entropy and sample entropy with short data sets. *Ann. Biomed. Eng.* 2012; 41: 349–365.5.

364 5. Richman JS, Moorman JR. Physiological time series analysis using approximate entropy and
365 sample entropy. *Am. J. Physiol.* 2000; 278: H2039–H2049.

366 6. Zandiyeh P, von Tscharner V. Reshape scale method: A novel multi scale entropic analysis
367 approach. *Physica A: Statistical Mechanics and its Applications.* 2013; 392: 6265-6272.

368 7. Hodson-Tole EF and Wakeling JM. Movement complexity and neuromechanical factors affect
369 the entropic half-life of myoelectric signals. *Front. Physiol.* 2017; 8: 3283.

370 8. Blake OM, Wakeling JM. Muscle Coordination Limits Efficiency and Power Output of Human
371 Limb Movement under a Wide Range of Mechanical Demands. *J Neurophysiol.* 2015; 114: 3283–3295

372 9. Ericson MO. On the biomechanics of cycling. A study of joint and muscle load during exercise
373 on the bicycle ergometer. *Scand J Rehabil Med Suppl.* 1986; 16: 1–43.

374 10. Ericson MO, Nisell R, Arborelius UP, Ekholm J. Muscular activity during ergometer cycling.
375 *Scand J Rehabil Med* 1985; 17: 53–61.

376 11. Hug F, Bendahan D, Le Fur Y, Cozzone PJ, Grelot L. Heterogeneity of muscle recruitment
377 pattern during pedaling in professional road cyclists: a magnetic resonance imaging and
378 electromyography study. *Eur J Appl Physiol.* 2004; 92: 334–342.

379 12. Jorge M, Hull ML. Analysis of EMG measurements during bicycle pedalling. *J Biomech.* 1986;
380 19: 683–694.

381 13. MacIntosh BR, Neptune RR, Horton JF. Cadence, power, and muscle activation in cycle
382 ergometry. *Med Sci Sports Exerc.* 2000; 32: 1281–1287.

383 14. Sarre G, Lepers R, Maffiuletti N, Millet G, Martin A. Influence of cycling cadence on
384 neuromuscular activity of the knee extensors in humans. *Eur J Appl Physiol.* 2003; 88: 476–479.

385 15. Wakeling JM, Horn T. Neuromechanics of muscle synergies during cycling. *J Neurophysiol.*
386 2009; 101: 843–854.

387 16. Wakeling JM. Patterns of motor recruitment can be determined using surface EMG. *J*
388 *Electromyogr Kinesiol.* 2009; 19, 199-207.

389 17. Wakeling JM, Uehli K, Rozitis AI. Muscle fibre recruitment can respond to the mechanics of the
390 muscle contraction. *J Roy Soc Interface* 2006; 3: 533-544.

391 18. Enders H, von Tscharner, V, Nigg, BM. Neuromuscular strategies during cycling at different
392 muscular demands. *Med. Sci. Sports Exerc.* 2015; 47: 1450–1459

393 19. Goldberger AL, Amaral LAN, Glass L, et al. PhysioBank, Physio- Toolkit, and PhysioNet:

components of a new research resource for complex physiologic signals. *Circulation.* 2000; 101(23):e215–20.

20. Richman JS, Lake DE, Moorman, JR (2004). Sample entropy. *Methods Enzymol* 2004; 384: 172-184.

21. von Tscharner V. Intensity analysis in time-frequency space of surface myoelectric signals by wavelets of specified resolution. *J. Electromyogr. Kinesiol.* 2000; 10, 433-445.

22. Oppenheim AV, Lim JS. The importance of phase in signals. *Proc IEEE.* 1981; 69: 529–541.

23. Karlsson S, Yu J, Akay M. Time–frequency analysis of myoelectric signals during dynamic contractions: a comparative study. *IEEE Trans Biomed Eng*. 2000; 47: 228–237.

24. Vaillancourt DE, Larsson L, Newell KM. Effects of aging on force variability, single motor unit discharge patterns, and the structure of 10, 20, and 40 Hz EMG activity. *Neurobiol Aging.* 2003; 24: 25–35.

25. Vaillancourt DE, Larsson L, Newell KM. Time-dependent structure in the discharge rate of human motor units. *Clin Neurophysiol.* 2002; 113:1325–1338.

26. Semmler JG, Sale MV, Meyer FG, Nordstrom MA. Motor-unit coherence and its relation with synchrony are influenced by training. *J Neurophysiol.* 2004; 92: 3320–3331.

27. Mueller H, Sternad D. Motor learning: changes in the structure of variability in a redundant task. *Adv Exp Med Biol.* 2009; 629: 439–456.

28. Enders H, Maurer C, Baltich J, Nigg BM. Task-oriented control of muscle coordination during cycling. *Med Sci Sports Exerc.* 2013; 45:2298–2305.

29. Baltich J, von Tscharner V, Zandiyeh P, Nigg BM. Quantification and reliability of center of pressure movement during balance tasks of varying difficulty. *Gait and Posture* 2014; 40: 327-332

30. Federolf P, Zandiyeh P, von Tscharner V. Time scale dependence of the center of pressure entropy: What characteristics of the neuromuscular postural control system influence stabilographic entropic half-life? *Exp Brain Res* 2015; 233: 3507-3515

31. Martin JC, Gardner AS, Barras M and Martin DT. Modeling sprint cycling using field-derived parameters and forward integration. *Med. Sci. Sports Exerc.* 2006; 38: 592–597

Figures

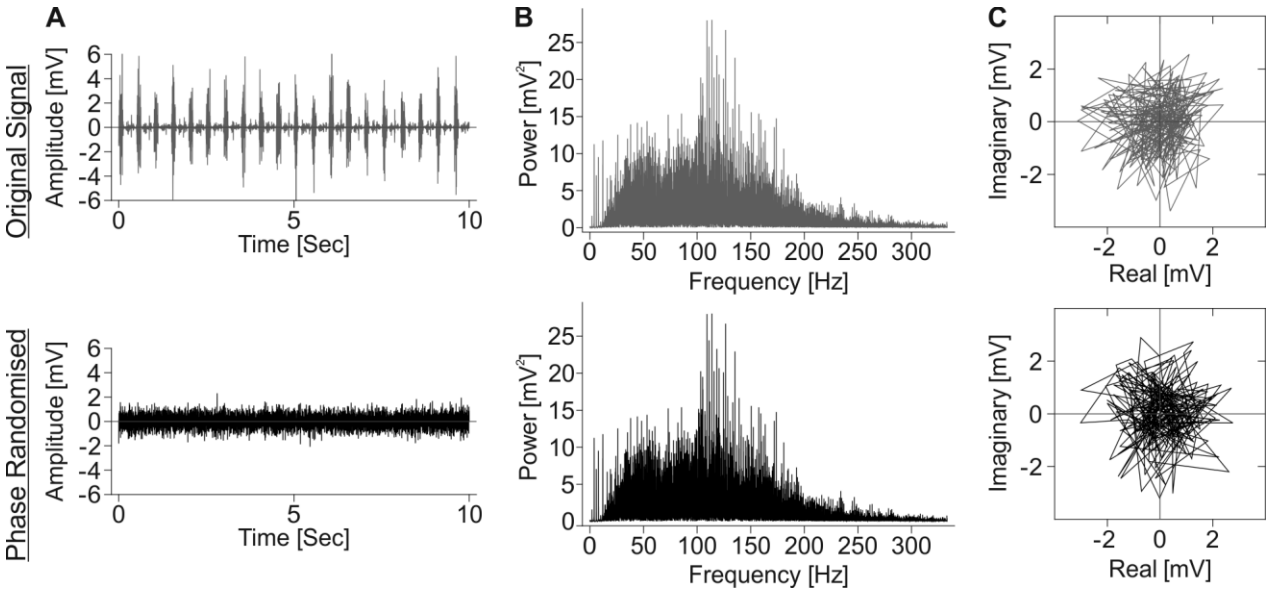

Fig. 1. Signal properties. Raw (top row) EMG shown in gray and phase-randomized surrogate (bottom row) signals shown in black. Time-varying signals (A), power spectra (B) and Argand diagrams showing the phase relations (C). Note that the power spectra (B) are the same for the raw signal and the phase-randomized surrogate. However, the signals have different phases (C) resulting in different burst characteristics as seen in the time-varying signals (A).

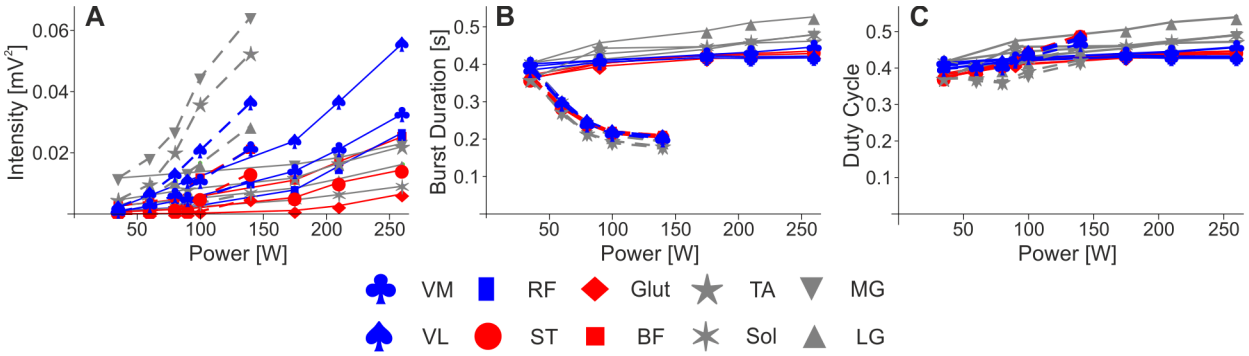

429

430 **Fig.2.** EMG intensity (A), burst duration (B) and duty cycle (C) for the different cycling conditions.

431 Cyclists pedalled at a low crank torque but increasing cadences (dashed lines), and at a low cadence but

432 increasing torque (solid lines). Each point represents the mean from 84 steady pedal cycles for nine

433 subjects.

434

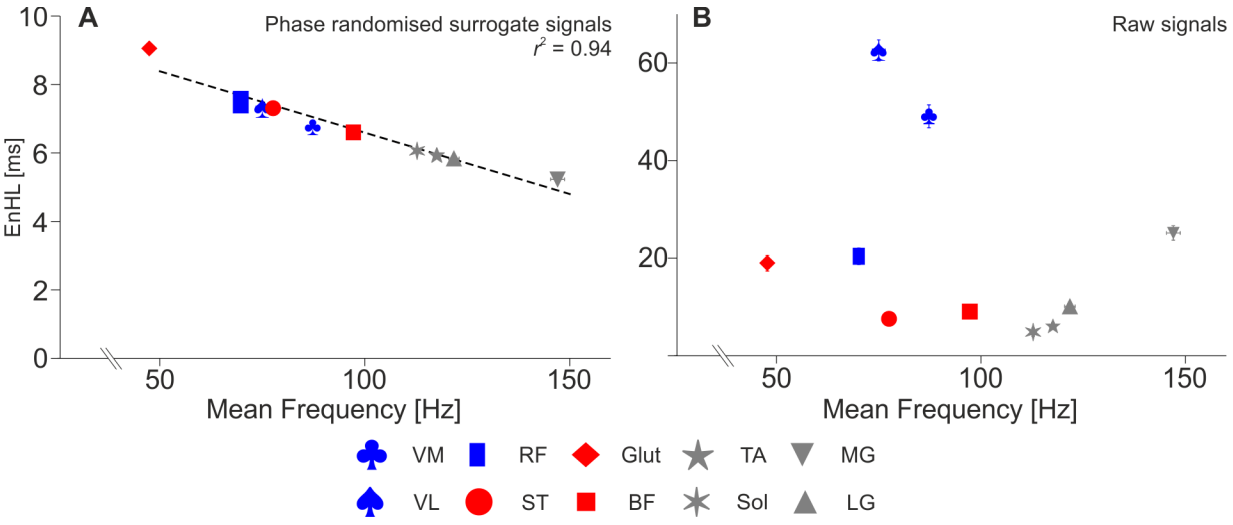

435

436 **Fig. 3.** Correlations of the entropic half-life EnHL with the mean frequency of the EMG for the phase-

437 randomized surrogate signals (A), and the raw EMG signals (B). Each point shows the mean ± S.E.M.

438 calculated across all nine subjects, nine pedal conditions and 3 blocks.

439

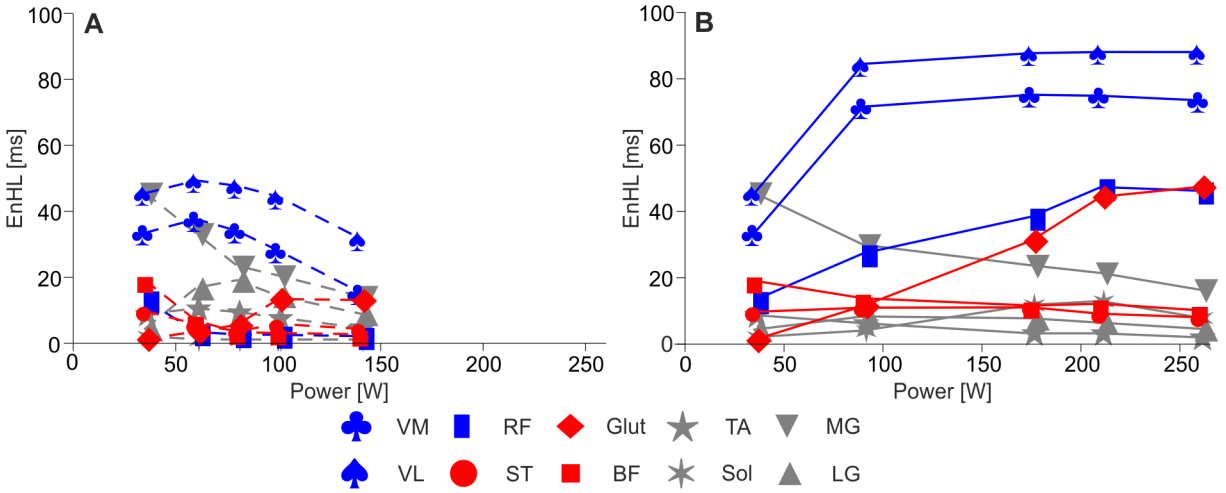

Fig. 4. Entropic half-lives EnHL for the raw EMG signals when cycling at a low crank torque but increasing cadences (A), and at a low cadence but increasing torque (B). The results of statistical analysis are shown in Table 1.

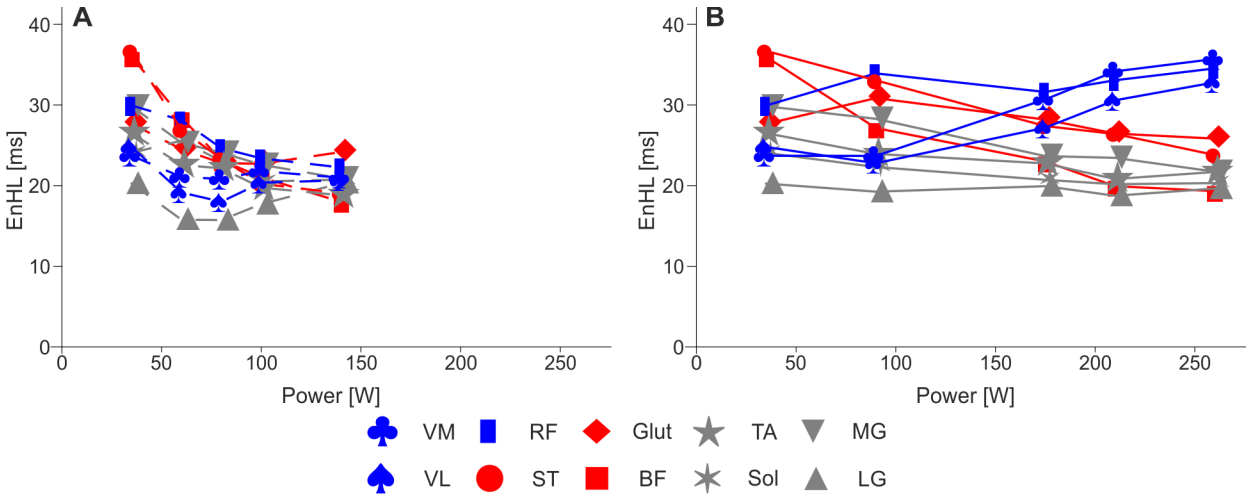

Fig. 5. Entropic half-lives EnHL for the EMG intensities when cycling at a low crank torque but increasing cadences (A), and at a low cadence but increasing torque (B). The results of statistical analysis are shown in Table 1.

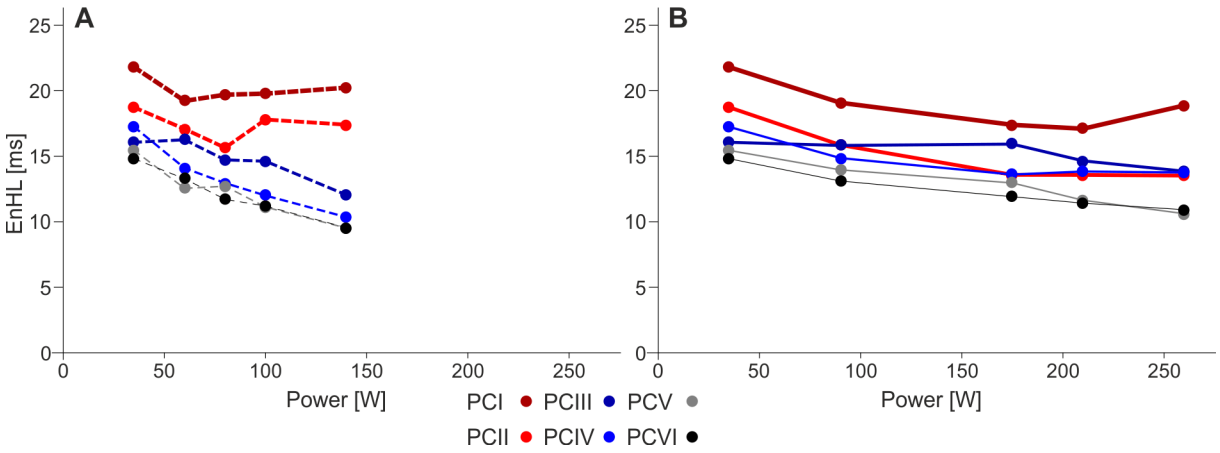

451

452 **Fig. 6.** Entropic half-lives EnHL for the PC loading scores for the muscle coordination when cycling at a

453 low crank torque but increasing cadences (A), and at a low cadence but increasing torque (B). The

454 results of statistical analysis are shown in Table 1.